HHS Public Access

Author manuscript

Brain Behav Immun. Author manuscript; available in PMC 2023 October 18.

Published in final edited form as:

Brain Behav Immun. 2022 August ; 104: 18–28. doi:10.1016/j.bbi.2022.05.007.

T-lymphocyte tyrosine hydroxylase regulates T_H17 T-lymphocytes during repeated social defeat stress

Safwan K. Elkhatib[a], **Cassandra M. Moshfegh**[a], **Gabrielle F. Watson**[a], **Adam J. Case**[b,c,*]

[a]Department of Cellular and Integrative Physiology, College of Medicine, University of Nebraska Medical Center, Omaha, Nebraska, United States

[b]Department of Psychiatry and Behavioral Sciences, Texas A&M Health Science Center, College Station, TX, United States

[c]Department of Medical Physiology, Texas A&M Health Science Center, College Station, TX, United States

Abstract

Posttraumatic stress disorder (PTSD) is a debilitating psychiatric disorder which results in deleterious changes to psychological and physical health. Patients with PTSD are especially susceptible to life-threatening co-morbid inflammation-driven pathologies, such as autoimmunity, while also demonstrating increased T-helper 17 (T_H17) lymphocyte-driven inflammation. While the exact mechanism of this increased inflammation is unknown, overactivity of the sympathetic nervous system is a hallmark of PTSD. Neurotransmitters of the sympathetic nervous system (*i.e.,* catecholamines) can alter T-lymphocyte function, which we have previously demonstrated to be partially mitochondrial redox-mediated. Furthermore, we have previously elucidated that T-lymphocytes generate their own catecholamines, and strong associations exist between tyrosine hydroxylase (TH; the rate-limiting enzyme in the synthesis of catecholamines) and pro-inflammatory interleukin 17A (IL-17A) expression within purified T-lymphocytes in a rodent model of psychological trauma. Therefore, we hypothesized that T-lymphocyte-generated catecholamines drive T_H17 T-lymphocyte polarization through a mitochondrial superoxide-dependent mechanism during psychological trauma. To test this, T-lymphocyte-specific TH knockout mice ($TH^{T\text{-}KO}$) were subjected to psychological trauma utilizing repeated social defeat stress (RSDS). RSDS characteristically increased tumor necrosis factor-α (TNFα), IL-6, IL-17A, and IL-22, however, IL-17A and IL-22 (T_H17 produced cytokines) were selectively attenuated in circulation and in T-lymphocytes of $TH^{T\text{-}KO}$ animals. When activated *ex vivo*, secretion of IL-17A and IL-22 by $TH^{T\text{-}KO}$ T-lymphocytes was also found to be reduced, but could be partially rescued with supplementation of norepinephrine specifically. Interestingly, $TH^{T\text{-}KO}$ T-lymphocytes were still able to polarize to T_H17 under exogenous polarizing conditions. Last,

*Corresponding author at: Department of Psychiatry and Behavioral Sciences, Department of Medical Physiology, College of Medicine, Texas A&M University, 3414 MREB2, 8447 Riverside Pkwy, Bryan, TX 77807, United States. acase@tamu.edu (A.J. Case).

Author Contributions

SKE and AJC conceptualized the overall investigation. SKE, CMM, GFW, and AJC designed all research methods and experimental studies. SKE, CMM, and GFW conducted experiments and analyzed data. SKE and AJC wrote the manuscript. All authors reviewed, edited, and approved the manuscript. AJC provided primary experimental oversight.

contrary to our hypothesis, we found RSDS-exposed $TH^{T\text{-}KO}$ T-lymphocytes still displayed elevated mitochondrial superoxide, suggesting increased mitochondrial superoxide is upstream of T-lymphocyte TH induction, activity, and T_H17 regulation. Overall, these data demonstrate TH in T-lymphocytes plays a critical role in RSDS-induced T_H17 T-lymphocytes and offer a previously undescribed regulator of inflammation in RSDS.

Keywords

PTSD; T-cell; Catecholamine; Superoxide; IL-17; IL-22; Cytokine

1. Introduction

Posttraumatic stress disorder (PTSD) is characterized by exposure to a traumatic event in conjunction with the persistence of a constellation of symptom clusters meeting specific diagnostic and statistical manual of mental disorders (DSM) criteria, such as affective changes, avoidance behavior, dissociative symptoms, and hyperarousal (APA, 2013). Importantly, there is a breadth of research demonstrating a connection between PTSD and deleterious changes to physical health (Ryder et al., 2018). Patients with PTSD are at an increased risk for a variety of inflammation-driven diseases, ranging from rheumatoid arthritis to cardiovascular disease (Boscarino et al., 2010; Mikuls et al., 2013; O'Donovan et al., 2015; Remch et al., 2018), which ultimately contribute to the decreased quality of life and lifespan of these patients. Intimately related to this risk for co-morbid diseases, patients with PTSD display distinctive physiological changes, specifically within the nervous and immune systems. Patients with PTSD demonstrate increased sympathetic tone by measures such as urinary norepinephrine (NE) and baroreflex sensitivity (Fonkoue et al., 2020; Park et al., 2017; Wingenfeld et al., 2015), in addition to heightened T-lymphocyte-driven inflammatory markers (Aiello et al., 2016; Maloley et al., 2019; Sommershof et al., 2009). There is a breadth of work demonstrating the effects of NE on T-lymphocyte functional status both *in vitro* and *in vivo* (Elkhatib and Case, 2019). For example, our *in vitro* work demonstrated NE supplementation to activated T-lymphocytes resulted in increased pro-inflammatory cytokine profiles, such as IL-6 and IL-17A, partially mediated by a mitochondrial redox mechanism (Case et al., 2016). Thus, the link between PTSD and inflammatory diseases may lie in connection of catecholamines and T-lymphocytes.

Critically, it has been shown in numerous investigations that catecholamines (dopamine, NE, and epinephrine) may be generated, released, and responded to by T-lymphocytes (Cosentino et al., 2007; Cosentino et al., 2002). This has been demonstrated at the single cell level in both isolated and immortalized lymphocytes, while *in vitro* studies utilizing pharmacological inhibition of catecholamine synthesis demonstrated these catecholamines influence the functionality and activation state of T-lymphocytes (Cosentino et al., 2007). In our own work, we investigated how increased sympathoexcitation in a murine model of psychological trauma known as repeated social defeat stress (RSDS) could affect T-lymphocyte inflammatory signatures (Moshfegh et al., 2019b). We discovered that T-lymphocytes from RSDS animals had increased gene expression of tyrosine hydroxylase (TH; the rate-limiting step in catecholamine synthesis), which strongly correlated with

expression of pro-inflammatory IL-17A in purified T-lymphocytes. Importantly, IL-17 and T_H17 cells have been heavily implicated in several inflammatory and autoimmune diseases as well as in the regulation of behavioral pathologies (Alves de Lima et al., 2020; Bedoya et al., 2013; Zambrano-Zaragoza et al., 2014), which suggests that T-lymphocyte produced catecholamines may play a currently undefined and critical role in the development of post-trauma pathophysiology.

To this end, we sought to examine the role of T-lymphocyte-generated catecholamines in the T-lymphocyte-driven inflammation seen during RSDS. RSDS has been extensively utilized to recapitulate various aspects of PTSD including increased arousal, depression-like behavior, social deficits, anhedonia, as well as increased systemic inflammation (Aspesi and Pinna, 2019; Deslauriers et al., 2018), and we have confirmed that this model consistently and reproducibly produces this phenotype (Elkhatib et al., 2020; Elkhatib et al., 2021; Moshfegh et al., 2019b). By generating a conditional T-lymphocyte TH knockout mouse ($TH^{T\text{-}KO}$), we were able to selectively investigate this mechanism and further define the role for catecholamines in T_H17-mediated inflammation.

2. Materials and methods

2.1. Mice

All experimental mice were bred inhouse in a room separate from stress induction and stress-exposed mice to reduce physical, psychological, and social stressors. Littermates were group housed (≤5 mice per cage) prior to RSDS or control protocol initiation at 8–12 weeks of age. All mice were housed with standard corncob bedding, paper nesting material, and given access to standard chow (Teklad Laboratory Diet #7012, Harlan Laboratories, Madison, WI) and water ad libitum. At the completion of experiments, experimental mice were euthanized by pentobarbital overdose (150 mg/kg, Fatal Plus, Vortech Pharmaceuticals, Dearborn, MI) administered by intraperitoneal injection. Daily RSDS and euthanasia occurred between 0700 and 1000 Central Standard Time to attenuate circadian rhythm effects on the neuroendocrine and immune systems.

In order to specifically investigate the role of TH in T-lymphocytes, a cell-type specific (conditional) TH knockout mouse was created and utilized herein. First, mice possessing loxP elements flanking exon 1 of the TH gene locus (*i.e.,* B6.Cg-$Th^{tm4.1\text{-}Rpa}$; $TH^{lox/lox}$) were graciously obtained from Michael Iuvone at Emory University (Jackson et al., 2012). $TH^{lox/lox}$ mice were then crossed to mice expressing codonimproved cre recombinase under the control of the distal promoter of T-lymphocyte-specific tyrosine kinase (Lck) (*i.e.,* B6.Cg-Tg(Lck-icre)$^{3779Nik/J}$), originally generated by Nigel Killeen (Zhang et al., 2005). This distal Lck promoter is active at or after T-cell receptor (TCR) upregulation during positive selection of thymocytes and has shown activity in both αβ and γδ T-lymphocyte subsets (Zhang et al., 2005). Mice were crossed to the F3 generation, allowing for 100% progeny possessing homozygous $TH^{lox/lox}$ alleles, 50% bearing Lck cre recombinase (Fig. 1A; T-lymphocyte specific TH knockouts; referred to as $TH^{T\text{-}KO}$), and 50% cre negative (Fig. 1A; $TH^{lox/lox}$ cre recombinase negative controls; referred to as TH^{Con}).

When possible, experimenters were blinded to the genotype and stress-exposure of mice until the completion of the study. Care was taken to blind experimenters to conditions during biological assay and data acquisition. All procedures were reviewed and approved by the University of Nebraska Medical Center and Texas A&M University Institutional Animal Care and Use Committees.

2.2. Genotyping TH KO

Rationally designed primers and polymerase chain reaction (PCR) were utilized to assess recombination of the TH gene. DNA was first isolated through use of GeneJET Genomic DNA Purification Kit (#K0722, Thermo scientific, Waltham, MA). Oligonucleotide primers (Forward: 5′-GAAGACCCTAGGGAGATGCCAAA-3′; Reverse 5′ TTTCCCTTACTTCA-CAAAATAGGACCCACAGAA) were specifically designed which could distinguish the recombined KO TH allele from the unperturbed $TH^{lox/lox}$ genotype by size. PCR products were loaded onto a 1.5% agarose gel with 1 mg/mL of ethidium bromide for intercalation, separated by electrophoresis at 100 V, and visualized under ultraviolet light alongside a DNA ladder (GeneRuler 1 kb Plus, #SM1331, Thermo Scientific).

2.3. Repeated social defeat stress paradigm

An adapted version of RSDS was performed as we have previous described (Elkhatib et al., 2020; Elkhatib et al., 2021; Moshfegh et al., 2019b). Briefly, RSDS exposes experimental mice to psychosocial trauma through repeated daily interaction and subsequent shared housing with 4–8-month-old aggressive, retired breeder mice of a CD-1 background (Charles River #022, Wilmington, MA). Due to usage of retired male breeders for stress induction, female mice and sex differences are precluded from study by conventional RSDS. During the 10-day RSDS paradigm, each experimental mouse was placed into the home cage of a CD-1 mouse for five minutes daily to allow for physical confrontation, while control mice remained in home cages. For the remaining 24 h, experimental and CD-1 mice were co-housed within the same cage but separated by a transparent, perforated barrier. This paradigm was repeated daily by rotating the experimental mouse to a novel CD-1 mouse and its respective cage, while control mice remained pair housed with other control mice throughout the duration of the RSDS paradigm. Mice were promptly excluded from further study if they demonstrated evident signs of wounding (>1 cm) or lameness during or after RSDS. At the end of the 10-day period (day 11), all mice underwent behavioral testing followed by euthanasia and tissue harvest the following day (day 12).

2.4. Elevated zero maze

In order to assess anxiety-like behavior, the elevated zero maze test was utilized as has been previously described (Moshfegh et al., 2019b). Briefly, the maze is comprised of a raised circular platform maze divided into quadrants, with two open portions and two closed arms. Following RSDS or control exposure, mice explore the novel environment for five minutes, with each session recorded and subsequently analyzed using Noldus Ethovision XT13 software (Noldus Information Technology).

2.5. Social interaction test

Following RSDS or control housing, pro-social and depressive-like behavior was assessed by the social interaction test as has been previously described (Moshfegh et al., 2019b). Briefly, each experimental mouse was placed within an open field chamber containing a small mesh enclosure in two separate 2.5-minute sessions. In the first session, all mice were tested with an empty enclosure. Next, a novel CD-1 mouse was placed within the enclosure and experimental mice were again recorded. All sessions were recorded, tracked, and analyzed with Noldus Ethovision XT13 software.

2.6. Splenic T-lymphocyte isolation

Pan, $CD4^+$, and $CD8^+$ murine T-lymphocytes were magnetically negatively selected from whole spleens as has been previously described (Case et al., 2016). Briefly, murine spleens were disassociated by ground glass slides, resuspended in supplemented RPMI media, then passed through a 70 μM filter. Splenic T-lymphocytes were isolated using EasySep Mouse T-cell Isolation Kit (#19851, STEMCELL™) per manufacturer's instructions. Enrichment of T-lymphocytes is regularly assessed by our lab with consistent purity > 90% based on CD3 + expression by flow cytometry.

2.7. T-lymphocyte activation, culture, and catecholamine supplementation

T-lymphocytes were cultured as has been previously described (Moshfegh et al., 2019a). Briefly, after T-lymphocyte isolation, 8.0×10^5 cells/mL were plated with anti-CD3/anti-CD28 magnetic activation beads in a 1:1 ratio with cells (Dynabeads™, #11456D, Thermo Fisher Scientific), and incubated for 72 h at 37 °C prior to harvest and analysis.

For catecholamine treatment conditions, freshly harvested splenic $CD4^+$ T-lymphocytes were isolated and plated in 24 well plates. Wells were supplemented daily with 10 μM of dopamine hydrochloride #AAA1113606, Thermo Scientific Chemicals), L-NE (#AAL0808703, Thermo Scientific Chemicals), or L-epinephrine (#AAL0491106, Thermo Scientific Chemicals) reconstituted in 1x sterile PBS. Catecholamine concentrations were based on our previous published work with *ex vivo* catecholamine dosage curves of T-lymphocytes (Case et al., 2016; Case and Zimmerman, 2015). T-lymphocytes from a single animal received each treatment condition allowing for paired analyses, with 3 technical replicates for each sample and treatment combination.

T-lymphocyte growth curves were obtained by live cell analyses. $CD4^+$ or $CD8^+$ T-lymphocytes were isolated and plated as stated above in 96-well flat bottom plates and then placed into an Incucyte S3 Live-cell analysis system (Essen Bioscience) housed within an environmental chamber (37 °C, 5% CO_2) for 72 h. Live cell images for confluence assessments were taken every 5 min for the 72-hour period. Confluence was normalized to starting densities after optical focusing, with > 5 technical replicate wells used per sample. Data were analyzed using Incucyte S3 analysis software.

2.8. T-lymphocyte T_H17 polarization

$CD4^+$ splenic T-lymphocytes were polarized to T_H17 *ex vivo* by use of CellXVivo Mouse Th17 Cell Differentiation Kit (#CDK017, R&D Systems). Briefly, $CD4^+$ T-

lymphocytes were isolated and cultured as described above with RPMI media additionally supplemented with a cocktail of proprietary polarizing reagent antibodies which promote T_H17 polarization and prevent T_H1 and T_H2 differentiation. Following 5 days of culture and activation, T-lymphocytes were harvested for flow cytometric staining and analysis.

2.9. Flow cytometric cellular staining

Extracellular and intracellular flow cytometric staining for T-lymphocyte populations was performed as has been previously described (Elkhatib et al., 2021). Briefly, cells were incubated at 37° C for 4 h in RPMI media supplemented with phorbol 12-myristate-13-acetate (PMA; 10 ng/mL), ionomycin (0.5 mg/mL), and BD GolgiPlug Protein Transport Inhibitor (containing brefeldin A; 1 mg/mL; BD Biosciences). Cells were washed, resuspended in PBS, and amine-reactive viability stained for 30 min at 4° C with Live/Dead Fixable Cell Stain Kit (#L34960, Thermo Fisher Scientific). Next, cells were washed and resuspended in RPMI media supplemented with antibodies targeting the following extracellular markers: CD3ε PE-Cy7 (clone 145–2C11, eBioscience), CD4 Alexa Fluor 488 (clone GK1.5, eBioscience), and CD8a APC (clone 53–6.7, BD Biosciences). In order to stain for intracellular proteins, cells were then fixed and permeabilized utilizing the FOXP3 Fixation and Permeabilization kit (#00–5523–00, eBioscience) per the manufacturer's instructions. Cells were washed again and resuspended for 30 min in permeabilization buffer containing IL-17A PE (clone TC11–18H10, BD Biosciences) and primary rabbit antityrosine hydroxylase antibody (clone EP1533Y, Abcam). Next, cells were washed and resuspended in RPMI media supplemented with secondary goat anti-rabbit QDOT 605 (Q11402MP, Invitrogen). Cells were then washed and resuspended in cold PBS for immediate analysis. Data were acquired using a customized BD LSRII flow cytometer (UNMC, BD Biosciences) or a 4-laser Attune NxT flow cytometer (Thermo Fisher Scientific). All flow cytometry experiments were completed with single-color and fluorescence minus one (FMO) control samples, with indirect intracellular staining also employing a primary antibody only control sample. All analyses were conducted on FlowJo 10 software (BD Bioscience).

2.10. Flow cytometric redox assessment

Mitochondrial-specific assessment of superoxide was performed as has been previously described (Case et al., 2016). Briefly, cells were stained with cell-type specific fluorescent antibodies [anti-CD3ε PE-Cy7 (clone 145–2C11, eBioscience), CD19 APC-Cy7 (clone 6D5, BioLegend), CD11b SB-436 (clone M1/70, eBioscience), CD11c APC (clone N418, eBioscience), and NK1.1 SB-600 (clone PK136, eBioscience)] in addition to 1 μM of (MATH) $O_2^{\cdot -}$-sensitive mitochondrial-localized probe, MitoSOX Red (#M36008, Thermo Fisher Scientific) for 30 min at 37 °C. Cells were analyzed on an LSRII flow cytometer at 488/610 nm excitation/emission, respectively, and data analyzed using FlowJo software.

2.11. RNA extraction, cDNA production, and real-time RT-qPCR

Gene expression assessment of purified T-lymphocytes was performed as previously described (Moshfegh et al., 2019b). Briefly, mRNA was extracted from purified T-lymphocytes by silica-membrane spin columns through use of RNAeasy mini kit

(#74104, Qiagen), then immediately converted to cDNA by High-Capacity cDNA Reverse Transcription Kit (#4374966, Applied Biosystems). Generated cDNA was used for real-time qPCR using respective gene targeted intronspanning gene-specific unlabeled primers and dual-labeled fluorescent FAM probes with a proprietary quencher molecule (PrimePCR™, Bio-Rad, Hercules, CA). Thresholds were set objectively to determine cycle thresholds (CT), with 40S ribosomal protein S18 (RPS18) utilized as a loading control to determine ΔCT. All values were normalized to TH^{Con} control samples to determine ΔCT values, which were then transformed to generate fold changes by the $2^{-\Delta\Delta CT}$ method.

2.12. Cytokine analyses

Plasma and spent culture media were harvested and analyzed for cytokine content by electrochemiluminescence as has been previously described (Elkhatib et al., 2020). Briefly, blood was harvested by cardiac puncture immediately following sacrifice and anticoagulated with EDTA. Plasma was separated by centrifugation and stored at −80 °C until assay. Spent media was harvested after 72 h of T-lymphocyte activation. First, antigenic activation beads were magnetically removed, followed by centrifugation at 500 × *g* for 2 min to pellet T-lymphocytes for downstream applications. Supernatant was removed and stored at −80 °C until assay. Cytokine analyses were conducted through use of U-PLEX T_H17 Meso Scale Discovery Kit (#K15078K, Meso Scale Discovery). All cytokine analyses were conducted per manufacturer's instructions and quantified on a Meso Scale Discovery Quickplex SQ 120, with analyses conducted using Mesoscale Discovery Workbench software.

2.13. Statistics

A total of 107 animals (53 TH^{Con}, 54 $TH^{T\text{-}KO}$) were utilized for the studies described herein. All data are presented as mean ± standard error of the mean (SEM) with sample numbers displayed as individual markers, same for repeated measures experiments, where n values are included within figure legend. Due to the nature of the experiments herein, not every biological assay was completed on each mouse within the RSDS or control paradigms. At least 3 independent experimental repeats were conducted for each experimental design. For comparisons with two independent groups, Shapiro-Wilk normality was performed followed by statistical testing by Mann-Whitney U or Student *t*-test as appropriate. In experiments with two levels of categorical variables (such as RSDS/Control, and TH^{Con}/$TH^{T\text{-}KO}$), full model two-way ANOVA was utilized. Two-way ANOVA Šidák multiple comparison tests of interest are listed in figures if respective group or interaction effects were found to be significant, with ANOVA p values listed within figure legend. All statistics were completed in GraphPad Prism (V9, GraphPad).

3. Results

3.1. $TH^{T\text{-}KO}$ mice are viable model to assess TH within T-lymphocytes

In order to investigate the role of TH in T-lymphocytes exclusively, a conditional knockout mouse was generated and validated (Fig. 1A). In Lck-driven cre-expressing cells (*i.e.,* T-lymphocytes), exon 1 of the TH gene was successfully removed, resulting in an ~ 800 bp shifted product by PCR (Fig. 1B). Due to the likely imperfect T-lymphocyte purification (on average achieve > 90% T-lymphocytes), faint non-recombined bands can be seen within

$TH^{T\text{-}KO}$ T-lymphocyte PCR products (Fig. 1B). Furthermore, flow cytometric assessment demonstrated nearly absent TH within T-lymphocytes from $TH^{T\text{-}KO}$ mice [$CD3\varepsilon^+$; p = 0.0038, Fig. 1C). Overall, these data demonstrate effective knockout of TH within pan T-lymphocytes of $TH^{T\text{-}KO}$ mice.

3.2. Behavioral responses to RSDS are not altered in $TH^{T\text{-}KO}$ mice

Following exposure to RSDS or control paradigms, TH^{Con} and $TH^{T\text{-}KO}$ mice were assessed for differences in sociability and anxiety-like behavior by social interaction test and elevated zero maze, respectively. By elevated zero maze, control $TH^{T\text{-}KO}$ mice demonstrated less distance moved after RSDS-exposure, independent of T-lymphocyte TH (p = 0.0059, TH^{Con} Con vs. RSDS, and p = 0.0067, $TH^{T\text{-}KO}$ Con vs. RSDS; Fig. 2A). Time within the open arm was significantly different by RSDS only (p = 0.0040, Two-way ANOVA), with multiple comparison tests nearing significance (p = 0.1114, TH^{Con} Con vs. RSDS, and p = 0.1114, $TH^{T\text{-}KO}$ Con vs. RSDS; Fig. 2A). From the social interaction ratio, RSDS-exposed TH^{Con} and $TH^{T\text{-}KO}$ mice demonstrated significant reductions in sociability (p = 0.0063, TH^{Con} Con vs. RSDS, and p = 0.0159, $TH^{T\text{-}KO}$ Con vs. RSDS; Fig. 2B), with no effect of genotype (p = 0.9233, Two-way ANOVA). These assessments demonstrate established behavioral changes following RSDS exposure, with TH expression in T-lymphocytes having no influence on these RSDS-induced behaviors.

3.3. Circulating T_H17 cytokines differ in $TH^{T\text{-}KO}$ mice after RSDS, reflecting changes in T_H17 populations and cytokine expression

We have previously demonstrated RSDS significantly increases circulating pro-inflammatory cytokines in WT mice, such as IL-2, IL-6, IL-10, IL-17A, IL-22, TNFα, CCL2, and CXCL2 (Elkhatib et al., 2020). Importantly, many of these cytokines are related to adaptive immune function and can be generated by T-lymphocytes. In particular, IL-17A and IL-22 are cytokines released in large quantities by T_H17 T-lymphocytes, a subtype of $CD4^+$ T-lymphocytes which have been implicated in autoimmunity (Bedoya et al., 2013). In TH^{Con} mice, RSDS induced a significant increase in many of these cytokines paralleling earlier studies, such as IL-6, TNFα, IL-17A, IL-22, and IL-10 despite smaller sample sizes across the four groups (p = 0.0429, 0.0011, 0.0001, 0.0040, and 0.0015, respectively, TH^{Con} Con vs. RSDS; Fig. 3A). In $TH^{T\text{-}KO}$ mice, IL-6, TNFα, and IL-10 in circulation were increased after RSDS (p = 0.0571, 0.0003, and 0.0016, respectively, $TH^{T\text{-}KO}$ Con vs. RSDS; Fig. 3A). However, this increase in RSDS-exposed $TH^{T\text{-}KO}$ mice was significantly attenuated in IL-17A and IL-22, specifically (p = 0.9662 and 0.9986, respectively, $TH^{T\text{-}KO}$ Con vs. RSDS; Fig. 3A), with differences in IL-17A and IL-22 by genotype in RSDS-exposed animals (p = 0.0009 and 0.0026, respectively, TH^{Con} RSDS vs. $TH^{T\text{-}KO}$ RSDS; Fig. 3A).

To further investigate these cytokine changes, splenic T-lymphocytes were isolated for gene expression analyses by real-time qPCR. We observed statistically significant increases in IL-6 and TNFα gene expression independent of genotype (p = 0.0292 and 0.0001, respectively, TH^{Con} Con vs. RSDS; p < 0.0001 and 0.0002, respectively, $TH^{T\text{-}KO}$ Con vs. RSDS) with no changes in IL-10 expression (Fig. 3B). However, we demonstrated a similar attenuation of RSDS-induced increases in expression of IL-17A and IL-22 in $TH^{T\text{-}KO}$

T-lymphocytes as compared to TH^{Con} T-lymphocytes ($p < 0.0001$ and 0.0098, respectively, TH^{Con} RSDS vs. $TH^{T\text{-}KO}$ RSDS; Fig. 3B).

We next investigated T_H17 populations in our $TH^{T\text{-}KO}$ mice and RSDS paradigms by a multi-parametric flow cytometric panel to identify T_H17 T-lymphocytes ($CD3\varepsilon^+CD4^+CD8^-IL\text{-}17A^+$ splenocytes; Fig. 4). RSDS induced an increase percentage of T_H17 T-lymphocytes in TH^{Con} mice but had had no effect on T_H17 percentages in $TH^{T\text{-}KO}$ mice ($p = 0.0251$, TH^{Con} Con vs. RSDS; $p > 0.9999$; $TH^{T\text{-}KO}$ Con vs. RSDS; Fig. 4), with significant differences in RSDS-exposed animals by genotype ($p = 0.0026$, TH^{Con} RSDS vs. $TH^{T\text{-}KO}$ RSDS; Fig. 4). When examining absolute numbers of splenic T_H17 lymphocytes, a similar trend to that of the percentages is observed. However, the number of $TH^{T\text{-}KO}$ T_H17 T-lymphocytes is significantly lower in baseline control conditions ($p = 0.0344$ TH^{Con} Con vs. $TH^{T\text{-}KO}$ Con; Fig. 4). Overall, these data demonstrate RSDS induces T_H17 polarization and IL-17A production in a TH-dependent fashion within T-lymphocytes.

3.4. $TH^{T\text{-}KO}$ T-lymphocytes demonstrate altered secretion of IL-17A and IL-22 despite similar growth

To focus our investigation on the role of TH in T-lymphocytes, $TH^{T\text{-}KO}$ $CD4^+$ and $CD8^+$ T-lymphocytes from control (unstressed) animals were isolated for culture and activated by antigen-independent anti-CD3/CD28 stimulatory beads. Utilizing live-cell imaging, we detected no differences in growth in $TH^{T\text{-}KO}$ $CD4^+$ or $CD8^+$ T-lymphocytes ($p = 0.6912$ and 0.3516, respectively; Fig. 5A). After 72 h of activation, cytokine analyses of spent media of $TH^{T\text{-}KO}$ $CD4^+$ T-lymphocytes revealed altered content of critical pro-inflammatory cytokines; IL-6 and TNFα were unchanged or trended towards statistical significance ($p = 0.8353$ and 0.0606, respectively; Fig. 5B) while IL-17A and IL-22 were significantly decreased ($p = 0.0040$ and 0.008, respectively; Fig. 5B). These cytokines were found unchanged or undetectable in $CD8^+$ T-lymphocyte culture media (data not shown). Overall, this investigation provides further evidence of differences in $TH^{T\text{-}KO}$ T-lymphocytes ability to produce T_H17 cytokines.

3.5. $TH^{T\text{-}KO}$ T-lymphocyte IL-17A and IL-22 cytokine production can be restored with catecholamine supplementation

To explore the role of specific catecholamines in TH^{Con} and $TH^{T\text{-}KO}$ $CD4^+$ T-lymphocyte cytokine production, $CD4^+$ T-lymphocytes were isolated, activated, and cultured *ex vivo* with 10 μM of each dopamine, NE, or epinephrine for paired analyses after 72 h. IL-17A and IL-22 production was rescued primarily by NE supplementation ($p = 0.7989$, TH^{Con} Vehicle vs. $TH^{T\text{-}KO}$ NE; Fig. 6A), with dopamine and epinephrine supplementation demonstrating modest effects. TNFα demonstrated no significant changes with catecholamine supplementation or by genotype (Fig. 6A). Overall, this further validates a role for T-lymphocyte TH and subsequent catecholamines in T_H17 salient cytokines.

3.6. T-lymphocyte TH is not necessary for ex vivo T_H17 polarization and does not function through a mitochondrial superoxide mechanism

We next investigated necessity versus sufficiency of T-lymphocyte TH in T_H17 polarization *ex vivo.* $CD4^+$ TH^{Con} and $TH^{T\text{-}KO}$ T-lymphocytes were isolated and cultured with T_H17

exogenous polarizing conditions. T_H17 polarization was evident by flow cytometric analysis after 5 days, with no observable changes between genotypes ($p = 0.8012$, Fig. 6B), suggesting T-lymphocytes can still polarize to T_H17 in the absence of TH if given a strong enough stimulus. Lastly, as we have previously shown a role for mitochondrial superoxide in T_H17 polarization (Case et al., 2016; Elkhatib et al., 2021; Moshfegh et al., 2019a), mitochondrial superoxide was assessed herein. Unexpectedly, mitochondrial superoxide was increased by RSDS in both TH^{Con} and $TH^{T\text{-}KO}$ T-lymphocytes ($p = 0.0020$, TH^{Con} Con vs. RSDS; $p = 0.0067$ $TH^{T\text{-}KO}$ Con vs. RSDS; Fig. 6C), implying an uncoupling of between T-lymphocyte TH mechanisms and the mitochondrial redox environment.

4. Discussion

Herein, we successfully generated a murine TH-deficient T-lymphocyte model to assess its role after psychological trauma. Firstly, we demonstrated the viability of $TH^{T\text{-}KO}$ mice and a successful reduction in TH in $TH^{T\text{-}KO}$ T-lymphocytes, while also finding patent RSDS-induced changes to anxiety-like or pro-social behavior in $TH^{T\text{-}KO}$ mice. This intriguing observation raises several questions regarding the relationship between inflammation and behavior. It is often presumed that the inflammatory and behavioral phenotypes of trauma and/or PTSD are tightly associated, however, this does not always appear to be the case. For example, Hodes *et al.* demonstrated that IL-6 displayed links between only social behavior in a model of RSDS (Hodes et al., 2014). This finding argues that certain cytokines are related to specific behavioral manifestations. This is further supported by the recent observation by Alves de Lima *et al.* that showed a role for IL-17A in anxiety-like behavior (Alves de Lima et al., 2020). We too have observed that specific sets of cytokines are linked to anxiety-like behavior after RSDS, with IL-17A also being detected in our dataset (Elkhatib et al., 2020). However, in this same dataset, we observed no associations between any cytokines and social behavior, and were unable to confirm and replicate the previous report from Hodes *et al.* (Elkhatib et al., 2020). Moreover, in a recent work where we utilized surgical denervation to remove sympathetic innervation to the spleen, we were able to reverse peripheral inflammation but not affect behavioral outcomes after RSDS (Elkhatib et al., 2021). While these data may seem conflicting, the contrasting results may simply be due to nuanced differences in experimental design. For example, Hodes *et al.* found that leukocyte stimulated IL-6 production was closer linked to social behavior than simply circulating levels of the cytokine as in our studies. Additionally, Alves de Lima *et al.* primarily examined the anxiety-like behavioral effects of centrally located IL-17A produced by γδ T-lymphocytes, as opposed to peripheral IL-17A generated by classic T_H17 lymphocytes that was studied herein. This difference between central and peripheral cytokine production may be vital in understanding inflammation, behavior, and the effects observed in the work presented here. It is well documented that cytokines play a significant role in nervous system development and function, and contribute to both behavior and learning (Mousa and Bakhiet, 2013; Vitkovic et al., 2000). Given that we examined the effects of TH loss in peripheral T-lymphocytes, it remains unknown if centrally located T-lymphocytes express TH or if they are affected in a similar manner to that of their peripheral counterparts. It is possible in our TH knock-out model that the cytokine milieu in the brain is unchanged, which may explain why no behavioral differences were noted.

Furthermore, it is possible that the Lck-Cre we utilized to knockout TH from T-lymphocytes only affected classic αβ subtypes as opposed to γδ. If indeed the IL-17A that regulates anxiety-like behavior is produced by centrally located γδ T-lymphocytes, then our knock-out which lowered IL-17A production from peripheral αβ T-lymphocytes would show little to no effect, which was observed. Additionally, while the loss of TH attenuated IL-17A production, it did not fully eliminate it. This may further explain why the loss of TH in T-lymphocytes had no effect on RSDS-induced behavioral outcomes.

The genesis for this investigation was based on a simple finding from our group (Moshfegh et al., 2019b). Across animals in both RSDS and control conditions, the gene expression of IL-17A and TH was strongly, positively correlated (R = 0.8722) in purified T-lymphocytes. Furthermore, RSDS increased expression of TH within T-lymphocytes. To test the potential causal relationship of these findings, we generated a conditional T-lymphocyte-specific knockout model of TH which is presented herein. While sparse, previous reports have identified catecholamine generation from T-lymphocytes, but have primarily focused on *in vitro*, pharmacological approaches. More recently, Yang *et al.* created a TH-deficient T-lymphocyte model using a ROR-γt promoter-driven cre recombinase after demonstrating a selective increase in the epinephrine and phenylethanolamine N-methyltransferase (PNMT; the synthetic enzyme preceding its production) in T_H17 polarized cells (Yang et al., 2021). After deleting TH in T-lymphocytes, they examined the phenotype of experimental autoimmune encephalitis (EAE), but interestingly did not observe any difference in clinical scores or lymphocyte infiltration into the CNS. Critically, EAE is an antigen-dependent response that develops after immunization by myelin basic protein, whereas RSDS-induced pro-inflammation and IL-17A is not known to be mediated through a single specific antigen, and may be a much weaker immune stimulus compared to an autoantigen. Additionally, much of the work by Yang *et al.* assessed the role of TH in T-lymphocytes through use of *in vitro* assays where T_H17 polarization was accomplished by exogenous administration of polarizing cytokines (*i.e.,* anti-IFN-γ, anti-IL-4, IL-6, TGFβ). In the work herein, we also demonstrate that T-lymphocyte TH is not necessary for exogenous, *ex vivo* T_H17 polarization. Together, our works provide valuable insights into the complex relationship between T-lymphocyte-derived catecholamines and T_H17 T-lymphocytes, with two differing disease models and approaches showing differential effects of TH loss.

Importantly, the exact mechanism that connects T-lymphocyte-generated catecholamines and T_H17 cells is still unknown. In our previous work, we have demonstrated the role for neuronally-derived NE in driving T_H17 profiles through a mitochondrial superoxide mechanism (Elkhatib et al., 2021). In that work, removal of neuron-produced NE caused an attenuation of mitochondrial superoxide and inflammatory state post-RSDS. This, along with our previous work showing attenuation of mitochondrial superoxide alone was sufficient to attenuate IL-6 and IL-17A production from T-lymphocytes treated with exogenous NE (Case et al., 2016), suggests that extracellular NE acting on T-lymphocytes works through redox mechanisms to regulate inflammation and polarization. However, the data presented herein indicates that T-lymphocyte mitochondrial superoxide operates upstream or in parallel of T-lymphocyte TH in inducing T_H17, since mitochondrial superoxide remained elevated after RSDS even in the absence of TH in T-lymphocytes. In other words, T-lymphocytes still were receiving the signal via RSDS to increase

mitochondrial superoxide production, and the loss of intracellular TH and catecholamine production had no impact on this redox mechanism but did have an impact on downstream cytokine production and polarization.

The loss of TH within T-lymphocytes would result in deficient production of all catecholamines, which canonically bind adrenergic receptors to influence T-lymphocyte functionality. There is a breadth of literature which has focused on the intracellular cascade that follows adrenergic receptor (AR) binding (Elkhatib and Case, 2019; Kin and Sanders, 2006; McAlees et al., 2011; Nance and Sanders, 2007; Sanders, 1995), and there are several potential pathways which could explain this relationship. In our work herein, we were able to rescue the attenuated *ex vivo* production of IL-17A and IL-22 by $TH^{T\text{-}KO}$ T-lymphocytes through primarily NE supplementation. This key observation helps understand the temporal nature of this signaling pathway. It is likely that stress through RSDS initiates the signaling cascade via neuronally-derived catecholamines, and thereafter T-lymphocytes induce TH and produce their own catecholamines for either autocrine or paracrine signaling necessary for IL-17A and IL-22 production. This elegant pathway may speculatively have evolved to eliminate the burden of signaling solely through the autonomic nervous system, and instead transfer the signaling and regulatory capacity on to the immune cells allowing them to self-regulate after the initial communication. While outside of the scope of this work, future work could serve to utilize various adrenergic α and β agonists and antagonists to further refine this pathway. We have attempted these types of studies in the past utilizing wild-type T-lymphocytes, but were hampered by the toxicity of combinational approaches, which limited conclusions (Case et al., 2016). A more refined approach in the future would be the development of conditional knockout animals that possess the ability to selectively remove all but one adrenergic receptor specifically in T-lymphocytes. Additionally, delineating the reception of T-lymphocyte-generated catecholamines specifically is an important future direction, especially giving special attention to non-canonical reception of catecholamines and intracellular signaling, as reviewed thoughtfully by Bellinger *et al.* (Lorton and Bellinger, 2015).

RSDS is an accepted murine model of psychological trauma which induces a robust T-lymphocyte inflammatory response (Elkhatib et al., 2020; Elkhatib et al., 2021; Moshfegh et al., 2019b). However, RSDS utilizes retired male breeder CD1 mice to induce psychological distress, and thus limited the inclusion of female mice herein. While models of RSDS have been developed which utilize females (Harris et al., 2018; Newman et al., 2019; Takahashi et al., 2017), many of these often utilize differential stress induction for the female mice, which introduces further variability and precludes direct comparison between male and female mice. As new rodent models that mimic aspects of PTSD, including systemic inflammation, are further developed and refined (Aspesi and Pinna, 2019; Deslauriers et al., 2018), examining the inflammatory and behavioral phenotype in $TH^{T\text{-}KO}$ is an important extension of these investigations to identify if the loss of TH in T-lymphocytes manifests differential outcomes in models that produce different phenotypes (e.g. HPA axis dysregulation, altered fear extinction retention, etc.). Additionally, cre recombinase in our experimentation was driven by the distal promoter of Lck in our model. This cre activation at the double positive ($CD4^+CD8^+$) thymocyte stage results in cre expression in all αβ T-lymphocytes (Zhang et al., 2005). Since this is relatively early in T-lymphocyte development, TH knockout at this

stage (and subsequent T_H17 dysregulation) could be the result of a developmental defect. The use of a conditional inducible T-lymphocyte promoter may shed additional insight onto this potential limitation.

Overall, this work provides new insights into the role for T-lymphocyte TH, specifically during psychological trauma. By utilizing an *in vivo* model, we were able to effectively demonstrate how T-lymphocyte-generated catecholamines are necessary for the T_H17-skewed inflammation seen during RSDS. Continued work investigating the mechanism of T-lymphocyte generated catecholamines, as well as their potential clinical relevance is an important future direction. By fully elucidating the nuance of these neuroimmune connections, we can further our understanding of fundamental T-lymphocyte biology and inflammation associated with PTSD.

Acknowledgements

This work was supported by the National Institutes of Health (NIH) R01HL158521 (AJC) and F30HL154535 (SKE).

Abbreviations:

PTSD	Post-traumatic stress disorder
DSM	The Diagnostic and Statistical Manual of Mental Disorders
TH	Tyrosine hydroxylase
NE	Norepinephrine
RSDS	Repeated social defeat stress

References

Aiello AE, Dowd JB, Jayabalasingham B, Feinstein L, Uddin M, Simanek AM, Cheng CK, Galea S, Wildman DE, Koenen K, Pawelec G, 2016. PTSD is associated with an increase in aged T cell phenotypes in adults living in Detroit. Psychoneuroendocrinology 67, 133–141. [PubMed: 26894484]

Alves de Lima K, Rustenhoven J, Da Mesquita S, Wall M, Salvador AF, Smirnov I, Martelossi Cebinelli G, Mamuladze T, Baker W, Papadopoulos Z, Lopes MB, Cao WS, Xie XS, Herz J, Kipnis J, 2020. Meningeal γδ T cells regulate anxiety-like behavior via IL-17a signaling in neurons. Nat. Immunol 21, 1421–1429. [PubMed: 32929273]

APA, 2013. Diagnostic and Statistical Manual of Mental Disorders

Aspesi D, Pinna G, 2019. Animal models of post-traumatic stress disorder and novel treatment targets. Behav. Pharmacol

Bedoya SK, Lam B, Lau K, Larkin J 3rd, 2013. Th17 cells in immunity and autoimmunity. Clin. Dev. Immunol 2013, 986789. [PubMed: 24454481]

Boscarino JA, Forsberg CW, Goldberg J, 2010. A twin study of the association between PTSD symptoms and rheumatoid arthritis. Psychosom. Med 72, 481–486. [PubMed: 20410244]

Case AJ, Zimmerman MC, 2015. Redox-regulated suppression of splenic T-lymphocyte activation in a model of sympathoexcitation. Hypertension 65, 916–923. [PubMed: 25691620]

Case AJ, Roessner CT, Tian J, Zimmerman MC, 2016. Mitochondrial superoxide signaling contributes to norepinephrine-mediated T-lymphocyte cytokine profiles. PLoS ONE 11, e0164609. [PubMed: 27727316]

Cosentino M, Marino F, Bombelli R, Ferrari M, Rasini E, Lecchini S, Frigo G, 2002. Stimulation with phytohaemagglutinin induces the synthesis of catecholamines in human peripheral blood mononuclear cells: role of protein kinase C and contribution of intracellular calcium. J. Neuroimmunol 125, 125–133. [PubMed: 11960648]

Cosentino M, Fietta AM, Ferrari M, Rasini E, Bombelli R, Carcano E, Saporiti F, Meloni F, Marino F, Lecchini S, 2007. Human CD4+CD25+ regulatory T cells selectively express tyrosine hydroxylase and contain endogenous catecholamines subserving an autocrine/paracrine inhibitory functional loop. Blood 109, 632–642. [PubMed: 16985181]

Deslauriers J, Toth M, Der-Avakian A, Risbrough VB, 2018. Current status of animal models of posttraumatic stress disorder: behavioral and biological phenotypes, and future challenges in improving translation. Biol. Psychiatry 83, 895–907. [PubMed: 29338843]

Elkhatib SK, Case AJ, 2019. Autonomic regulation of T-lymphocytes: implications in cardiovascular disease. Pharmacol. Res 146, 104293. [PubMed: 31176794]

Elkhatib SK, Moshfegh CM, Watson GF, Case AJ 2020. Peripheral inflammation is strongly linked to elevated zero maze behavior in repeated social defeat stress. Brain Behav. Immun

Elkhatib SK, Moshfegh CM, Watson GF, Schwab AD, Katsurada K, Patel KP, Case AJ, 2021. Splenic denervation attenuates repeated social defeat stress-induced T lymphocyte inflammation. Biol. Psychiatry: Global Open Sci 1, 190–200.

Fonkoue IT, Marvar PJ, Norrholm S, Li Y, Kankam ML, Jones TN, Vemulapalli M, Rothbaum B, Bremner JD, Le NA, Park J, 2020. Symptom severity impacts sympathetic dysregulation and inflammation in post-traumatic stress disorder (PTSD). Brain Behav. Immun 83, 260–269. [PubMed: 31682970]

Harris AZ, Atsak P, Bretton ZH, Holt ES, Alam R, Morton MP, Abbas AI, Leonardo ED, Bolkan SS, Hen R, Gordon JA, 2018. A novel method for chronic social defeat stress in female mice. Neuropsychopharmacology 43, 1276–1283. [PubMed: 29090682]

Hodes GE, Pfau ML, Leboeuf M, Golden SA, Christoffel DJ, Bregman D, Rebusi N, Heshmati M, Aleyasin H, Warren BL, Lebonte B, Horn S, Lapidus KA, Stelzhammer V, Wong EH, Bahn S, Krishnan V, Bolanos-Guzman CA, Murrough JW, Merad M, Russo SJ, 2014. Individual differences in the peripheral immune system promote resilience versus susceptibility to social stress. PNAS 111, 16136–16141. [PubMed: 25331895]

Jackson CR, Ruan GX, Aseem F, Abey J, Gamble K, Stanwood G, Palmiter RD, Iuvone PM, McMahon DG, 2012. Retinal dopamine mediates multiple dimensions of light-adapted vision. J. Neurosci 32, 9359–9368. [PubMed: 22764243]

Kin NW, Sanders VM, 2006. It takes nerve to tell T and B cells what to do. J. Leukoc. Biol 79, 1093–1104. [PubMed: 16531560]

Lorton D, Bellinger DL, 2015. Molecular mechanisms underlying beta-adrenergic receptor-mediated cross-talk between sympathetic neurons and immune cells. Int. J. Mol. Sci 16, 5635–5665. [PubMed: 25768345]

Maloley PM, England BR, Sayles H, Thiele GM, Michaud K, Sokolove J, Cannon GW, Reimold AM, Kerr GS, Baker JF, Caplan L, Case AJ, Mikuls TR, 2019. Post-traumatic stress disorder and serum cytokine and chemokine concentrations in patients with rheumatoid arthritis. Semin. Arthritis Rheum

McAlees JW, Smith LT, Erbe RS, Jarjoura D, Ponzio NM, Sanders VM, 2011. Epigenetic regulation of beta2-adrenergic receptor expression in T(H)1 and T(H)2 cells. Brain Behav. Immun 25, 408–415. [PubMed: 21047549]

Mikuls TR, Padala PR, Sayles HR, Yu F, Michaud K, Caplan L, Kerr GS, Reimold A, Cannon GW, Richards JS, Lazaro D, Thiele GM, Boscarino JA, 2013. Prospective study of posttraumatic stress disorder and disease activity outcomes in US veterans with rheumatoid arthritis. Arthritis Care Res. (Hoboken) 65, 227–234. [PubMed: 22740431]

Moshfegh CM, Collins CW, Gunda V, Vasanthakumar A, Cao JZ, Singh PK, Godley LA, Case AJ, 2019a. Mitochondrial superoxide disrupts the metabolic and epigenetic landscape of CD4(+) and CD8(+) T-lymphocytes. Redox Biol 101141. [PubMed: 30819616]

Moshfegh CM, Elkhatib SK, Collins CW, Kohl AJ, Case AJ, 2019b. Autonomic and redox imbalance correlates with T-lymphocyte inflammation in a model of chronic social defeat stress. Front. Behav. Neurosci 13, 103. [PubMed: 31139062]

Mousa A, Bakhiet M, 2013. Role of cytokine signaling during nervous system development. Int. J. Mol. Sci 14, 13931–13957. [PubMed: 23880850]

Nance DM, Sanders VM, 2007. Autonomic innervation and regulation of the immune system (1987–2007). Brain Behav. Immun 21, 736–745. [PubMed: 17467231]

Newman EL, Covington HE, Suh J, Bicakci MB, Ressler KJ, DeBold JF, Miczek KA, 2019. Fighting females: neural and behavioral consequences of social defeat stress in female mice. Biol. Psychiatry

O'Donovan A, Cohen BE, Seal KH, Bertenthal D, Margaretten M, Nishimi K, Neylan TC, 2015. Elevated risk for autoimmune disorders in iraq and afghanistan veterans with posttraumatic stress disorder. Biol. Psychiatry 77, 365–374. [PubMed: 25104173]

Park J, Marvar PJ, Liao P, Kankam ML, Norrholm SD, Downey RM, McCullough SA, Le NA, Rothbaum BO, 2017. Baroreflex dysfunction and augmented sympathetic nerve responses during mental stress in veterans with post-traumatic stress disorder. J. Physiol 595, 4893–4908. [PubMed: 28503726]

Remch M, Laskaris Z, Flory J, Mora-McLaughlin C, Morabia A, 2018. Post-traumatic stress disorder and cardiovascular diseases: a cohort study of men and women involved in cleaning the debris of the world trade center complex. Circ. Cardiovasc. Qual. Outcomes 11, e004572. [PubMed: 29991645]

Ryder AL, Azcarate PM, Cohen BE, 2018. PTSD and physical health. Curr. Psychiatry Rep 20, 116. [PubMed: 30367276]

Sanders VM, 1995. The role of adrenoceptor-mediated signals in the modulation of lymphocyte function. Adv. Neuroimmunol 5, 283–298. [PubMed: 8748072]

Sommershof A, Aichinger H, Engler H, Adenauer H, Catani C, Boneberg EM, Elbert T, Groettrup M, Kolassa IT, 2009. Substantial reduction of naive and regulatory T cells following traumatic stress. Brain Behav. Immun 23, 1117–1124. [PubMed: 19619638]

Takahashi A, Chung JR, Zhang S, Zhang H, Grossman Y, Aleyasin H, Flanigan ME, Pfau ML, Menard C, Dumitriu D, Hodes GE, McEwen BS, Nestler EJ, Han MH, Russo SJ, 2017. Establishment of a repeated social defeat stress model in female mice. Sci. Rep 7, 1283–1288. [PubMed: 28455520]

Vitkovic L, Konsman JP, Bockaert J, Dantzer R, Homburger V, Jacque C, 2000. Cytokine signals propagate through the brain. Mol. Psychiatry 5, 604–615. [PubMed: 11126391]

Wingenfeld K, Whooley MA, Neylan TC, Otte C, Cohen BE, 2015. Effect of current and lifetime posttraumatic stress disorder on 24-h urinary catecholamines and cortisol: results from the Mind Your Heart Study. Psychoneuroendocrinology 52, 83–91. [PubMed: 25459895]

Yang P, Tian H, Zou YR, Chambon P, Ichinose H, Honig G, Diamond B, Kim SJ, 2021. Epinephrine production in Th17 cells and experimental autoimmune encephalitis. Front. Immunol 12, 616583. [PubMed: 33692790]

Zambrano-Zaragoza JF, Romo-Martinez EJ, Duran-Avelar Mde J, Garcia-Magallanes N, Vibanco-Perez N, 2014. Th17 cells in autoimmune and infectious diseases. Int. J. Iinflam 2014, 651503.

Zhang DJ, Wang Q, Wei J, Baimukanova G, Buchholz F, Stewart AF, Mao X, Killeen N, 2005. Selective expression of the Cre recombinase in late-stage thymocytes using the distal promoter of the Lck gene. J. Immunol 174, 6725–6731. [PubMed: 15905512]

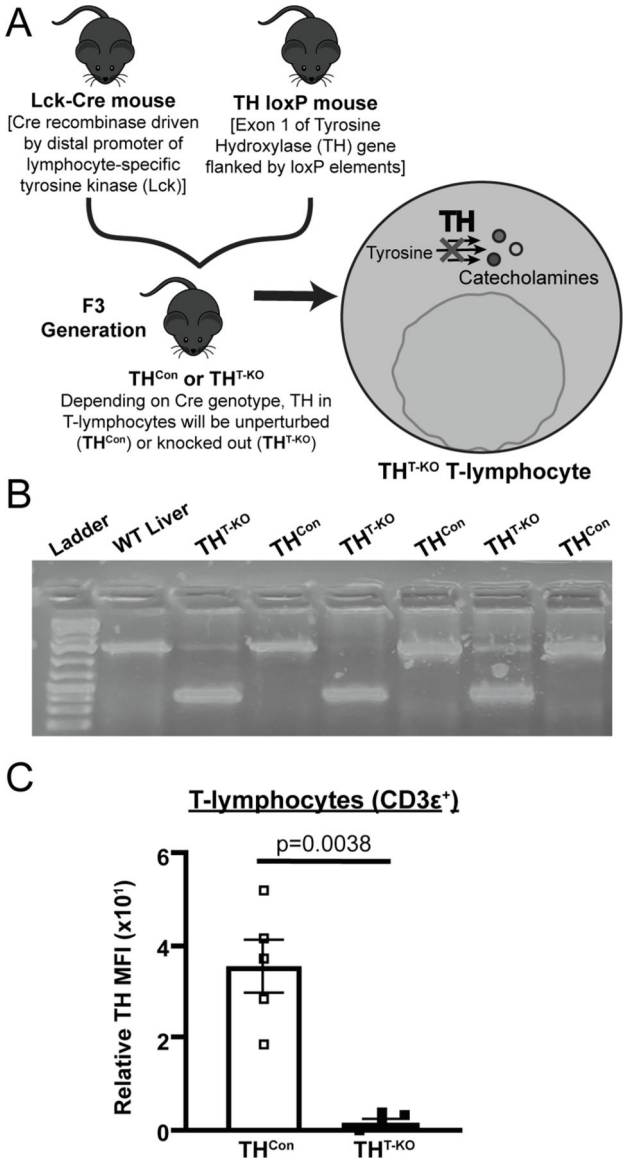

Fig. 1.

Generation and validation of a conditional T-lymphocyte TH knockout model. A) Through crossing of TH loxP and Lck-cre mice to the F3 generation, 50% conditional genetic knockout ($TH^{T\text{-}KO}$) and 50% cre-negative (TH^{Con}) mice were generated, allowing for *in vivo* investigation of the role of TH within T-lymphocytes was generated. B) Representative DNA gel of respective samples following PCR amplification with oligonucleotide primers which produced differentially sized PCR products. C) Quantification of flow cytometry of TH mean fluorescence intensity (MFI) in splenic T-lymphocytes (CD3ε+) in $TH^{T\text{-}KO}$ and TH^{Con} (N = 5 for each genotype); significance by Mann-Whitney *U* test, all values normalized to TH FMO tube.

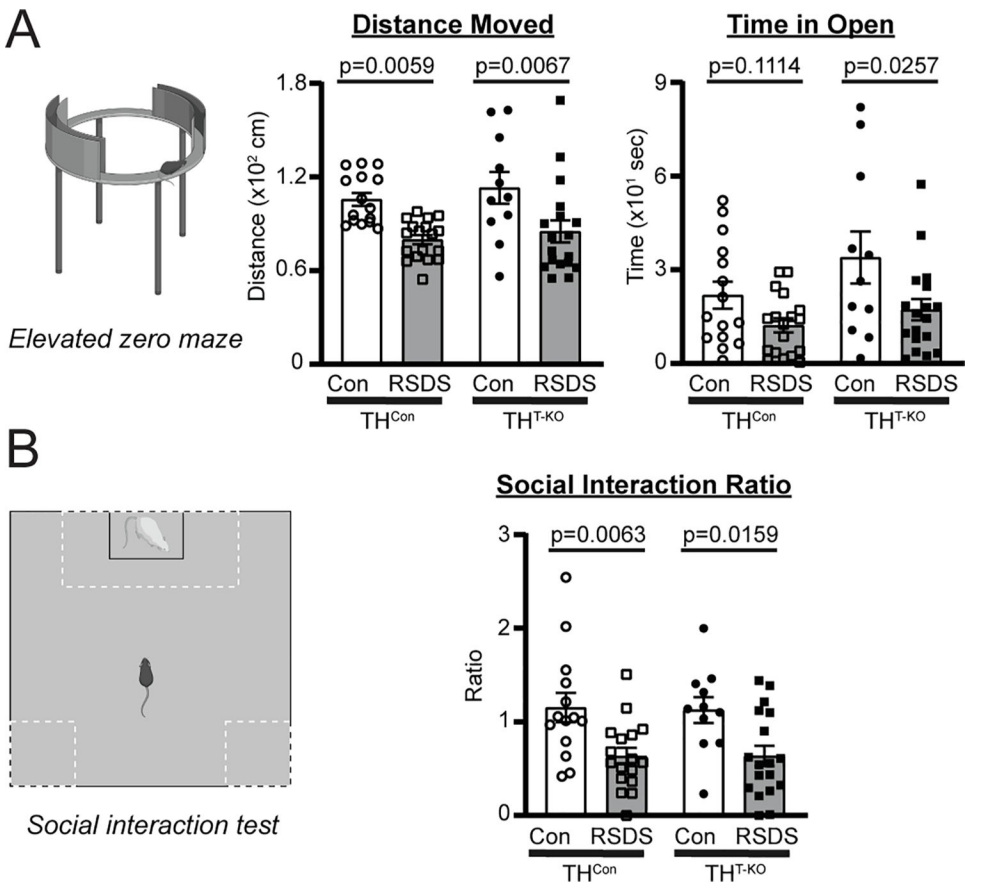

Fig. 2.

T-lymphocyte TH knockout does not affect RSDS-induced anxiety-like or social behavior. Mice were tested for anxiety-like and pro-social behavior following control or RSDS paradigms. A) *Left,* Representation of elevated zero maze for anxiety-like behavior. *Middle*, Total distance moved on elevated zero maze, Two-way ANOVA results; stress $p < 0.0001$, genotype $p = 0.3042$, interaction $p = 0.8672$. *Right*, Time in open arm of elevated zero maze, Two-way ANOVA results; stress $p = 0.0040$, genotype $p = 0.0575$, interaction $p = 0.4305$. B) *Left,* Representation of social interaction test for social behavior. *Right,* Social interaction ratio (defined as time spent with CD-1 present/time spent with empty enclosure), Two-way ANOVA results; stress $p = 0.0001$, genotype $p = 0.9233$, interaction $p = 0.9101$. N = 15, 18, 11, 18 for respective genotypes and treatments in each panel. Two-way ANOVA Šidák multiple comparison tests of interest are listed if respective group or interaction effects were found to be significant.

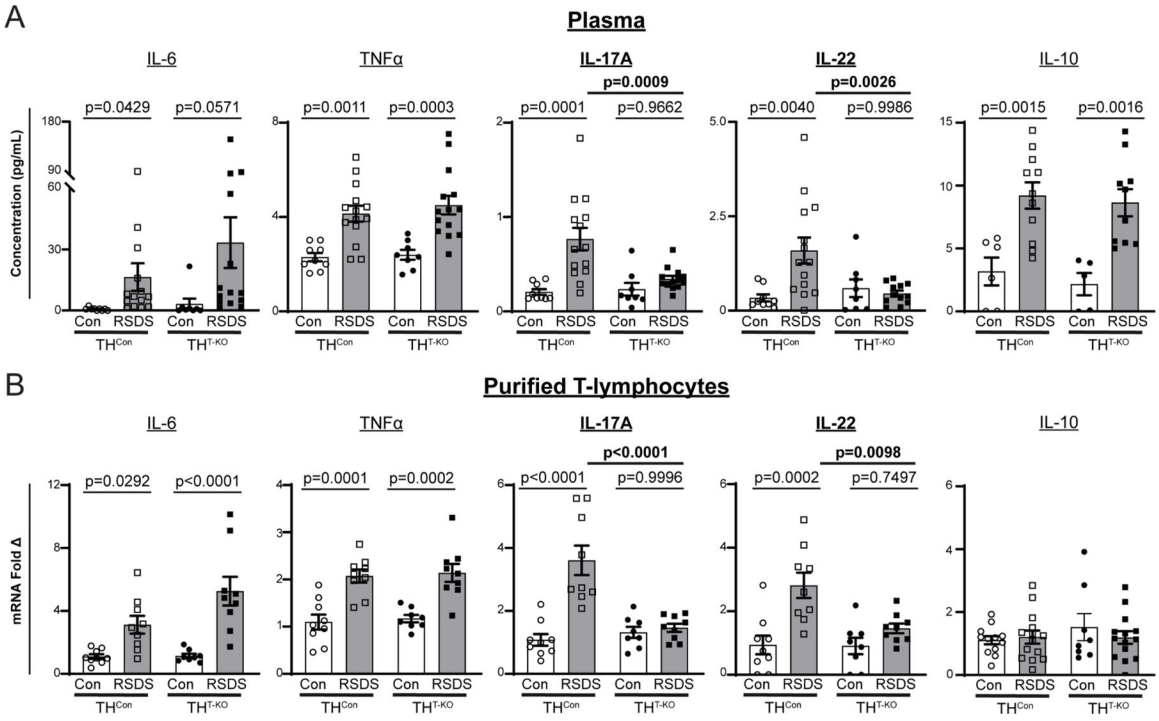

Fig. 3.

T-lymphocyte TH knockout selectively attenuates IL-17A and IL-22 cytokine levels. A) Circulating cytokines were assessed following control or RSDS paradigms with Meso Scale Discovery T_H17 (Combo 2) assay. IL-6 Two-way ANOVA results, Stress p = 0.0173, genotype p = 0.2997, interaction 0.4460; TNFα Two-way ANOVA results, Stress p < 0.0001, genotype p = 0.5229, interaction 0.7110; IL-17A Two-way ANOVA results, Stress p = 0.0004, genotype p = 0.0213, interaction p = 0.0089; IL-22 Two-way ANOVA results, Stress p = 0.0304, genotype p = 0.0442, interaction 0.0065. N = 9, 8, 14, 14 for respective genotypes and treatments. B) Splenic T lymphocytes were isolated by magnetic negative selection, followed by RNA extraction, cDNA conversion, and real-time qPCR. All ΔCT values normalized to 40S ribosomal protein S18 (RPS18) control, then fold change normalized to TH^{Con} Control animals. IL-6 Two-way ANOVA results, Stress p < 0.0001, genotype p = 0.0619, interaction 0.0733; TNFα Two-way ANOVA results, Stress p < 0.0001, genotype p = 0.6486, interaction 0.9768; IL-17A Two-way ANOVA results, Stress p < 0.0001, genotype p = 0.0019, interaction p = 0.0002; IL-22 Two-way ANOVA results, Stress p = 0.0001, genotype p = 0.0190, interaction 0.0200. N = 9, 8, 9, 9 for respective genotypes and treatments. Two-way ANOVA Šidák multiple comparison tests of interest are listed if respective group or interaction effects were found to be significant.

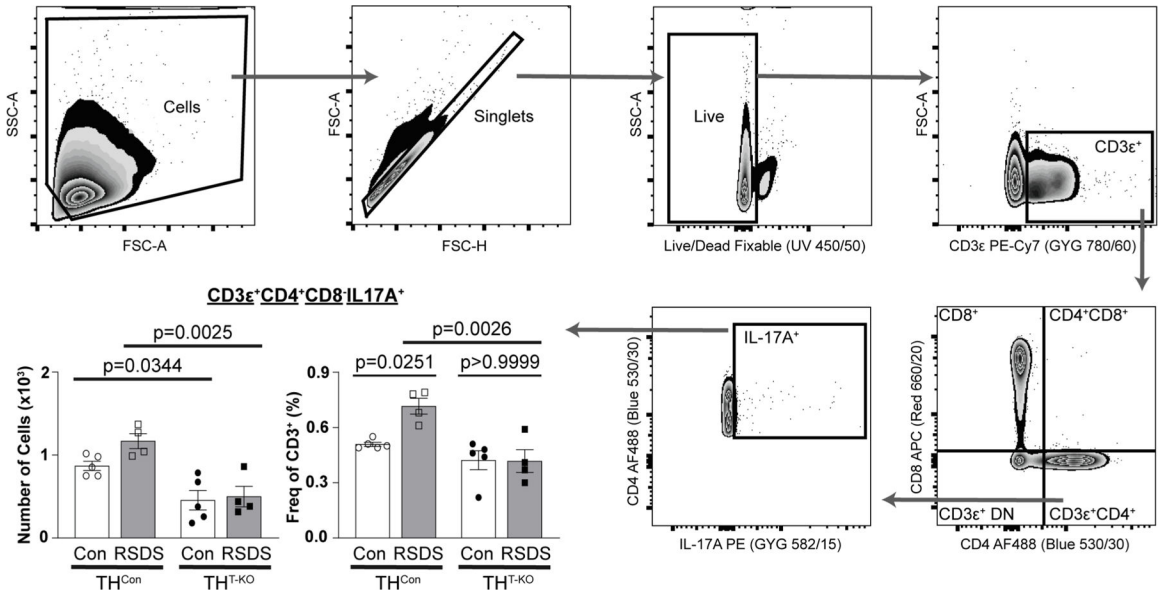

Fig. 4.

$TH^{T\text{-}KO}$ animals have attenuated T_H17 polarization following RSDS. Following RSDS or control paradigms, splenocytes were harvested for multiparametric flow cytometry for T_H17 T-lymphocytes ($CD3\varepsilon^+CD4^+CD8^-IL\text{-}17A^+$). Hierarchical gating strategy was employed to assess viability, percentage, and number of T_H17 positivity. N = 5, 4, 5, 4 for respective genotypes and treatments. Two-way ANOVA Šidák multiple comparison tests of interest are listed if respective group or interaction effects were found to be significant.

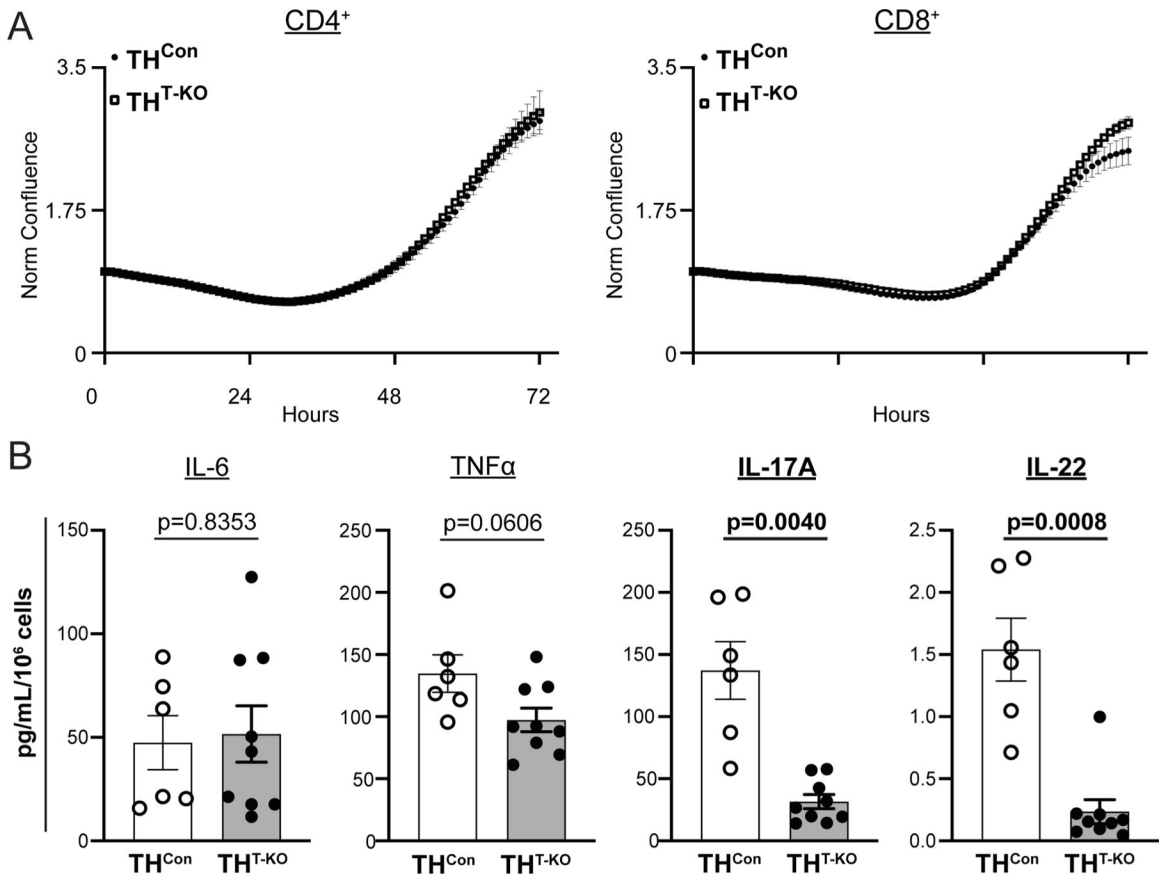

Fig. 5.

$TH^{T\text{-}KO}$ $CD4^+$ T-lymphocytes demonstrate altered T_H17 cytokine secretion, but similar growth. A) $CD4^+$ or $CD8^+$ T-lymphocytes were isolated by negative selection, plated with anti-CD3/CD28 beads, and imaged for confluence 72 h. N = 4 samples, with > 5 technical replicates per well. $CD4^+$ Repeated measures Two-way ANOVA results, Genotype p = 0.6912, Time p < 0.0001, Interaction p > 0.9999; $CD8^+$ Repeated measures Two-way ANOVA results, Genotype p = 0.3516, Time p = 0.0003, Interaction p = 0.0002. B) $CD4^+$ T-lymphocytes were isolated and activated as above, with spent culture media collected and assessed for cytokines by Meso Scale Discovery T_H17 (Combo 2) assay, with concentrations normalized to final cell counts. N = 6, 9 for respective genotypes. Listed p values were calculated by unpaired *t*-test (IL-6, TNFα, and IL-17A) or Mann-Whitney *U* test (IL-22) where appropriate from Shapiro-Wilk normality testing.

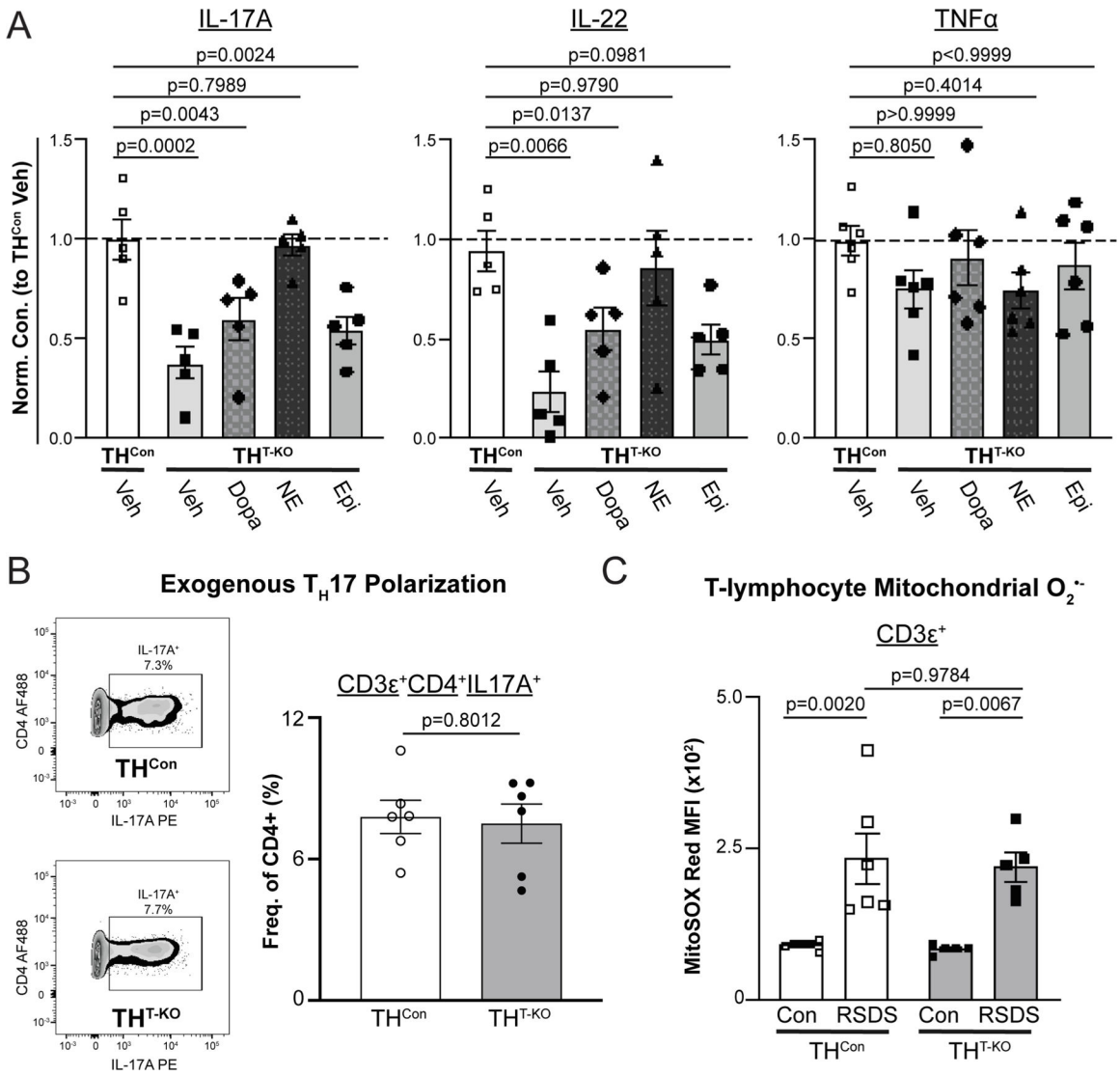

Fig. 6.

T_H17 cytokine production can be rescued with catecholamine supplementation, but T-lymphocyte TH is not necessary for T_H17 polarization, nor does it rely on mitochondrial redox. A) $CD4^+$ T-lymphocytes were isolated and activated with 10 μM of respective catecholamines supplemented. After 72 h, spent culture media was collected and assessed for cytokines by Meso Scale Discovery T_H17 (Combo 2) assay. Cytokine concentrations are normalized to TH^{Con} and final cell counts. N = 5 for respective genotypes and treatments. P-values represent nonparametric, paired measures ANOVA multiple comparisons tests (Friedman) compared to TH^{Con} vehicle. B) $CD4^+$ T-lymphocytes were isolated, activated, and cultured under T_H17 polarizing conditions for 5 days, then analyzed by flow cytometry. *Left,* Representative zebra plot. *Right,* TH17 T-lymphocytes following polarization; p-value by unpaired *t*-test. N = 6, 6 for respective genotypes. C) Following RSDS or control-housing exposure, splenic T-lymphocytes (CD3ε+) were stained with MitoSox Red to assess

mitochondrial superoxide levels. N = 6, 6, 5, 5 for respective genotypes and treatments. Two-way ANOVA results, Stress $p < 0.0001$, Genotype $p = 0.7096$, Interaction $p = 0.8952$.